

Highly efficient four-wave mixing in double- Λ system in ultraslow propagation regime

Ying Wu^{1,2} and Xiaoxue Yang¹

¹State Key Laboratory for Laser Technique and Physics Department, Huazhong University of Science and Technology, Wuhan 430074, People's Republic of China

²Center for Cold Atom Physics, The Chinese Academy of Sciences, Wuhan 430071, People's Republic of China

(Received 18 May 2004; revised manuscript received 20 August 2004; published 18 November 2004)

We perform a time-dependent analysis of four-wave mixing (FWM) in a double- Λ system in an ultraslow-propagation regime and obtain the analytical expressions of pulsed probe laser, FWM-generated pulse, phase shifts and absorption coefficients, group velocities, and FWM efficiency. With these analytical expressions, we show that an efficiently generated FWM field can acquire the same ultraslow group velocity ($V_g/c \sim 10^{-4} - 10^{-5}$) and pulse shape of a probe pump and that the maximum FWM efficiency is greater than 25%, which is orders of magnitude larger than previous FWM schemes in the ultraslow-propagation regime.

DOI: 10.1103/PhysRevA.70.053818

PACS number(s): 42.50.Gy, 32.80.Qk, 42.50.Hz

Multiwave mixing processes in the ultraslow-propagation regime have been the focus of several recent studies because of their potential wide range of applications in diverse fields such as high-efficiency generation of short-wavelength coherent radiation at pump intensities approaching the single-photon level, nonlinear spectroscopy at very low light intensity, quantum single-photon nonlinear optics, and quantum information science [1–25]. One of the major problems of multiwave mixing in the ultraslow-propagation regime is its low efficiency, usually smaller than 0.1% for four-wave mixing in the ultraslow-propagation regime [3,4], which limits somewhat its applications. It is thus desirable to search for new efficient multiwave mixing schemes or approaches.

In this paper, we consider four-wave mixing (FWM) in a double- Λ system as shown in Fig. 1, where lifetime-broadened four-state atoms interact with two continuous-wave (cw) laser pump fields (c, d) and a weak-pulsed probe laser p , and a pulsed FWM field m can then be generated efficiently. Such a FWM scheme with all four waves considered as cw waves has been intensively studied previously

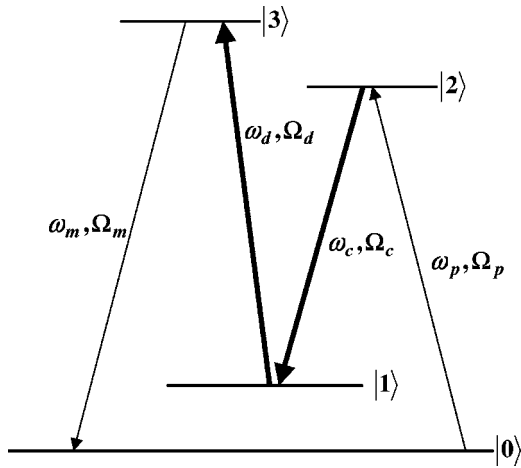


FIG. 1. Schematic of FWM in a double- Λ system. Lifetime-broadened four-level atoms interact with two cw laser pump fields (frequencies ω_c and ω_d and Rabi frequencies $2\Omega_c$ and $2\Omega_d$) and a weak pulsed probe pump (frequency ω_p and Rabi frequency $2\Omega_p$) to generate a FWM-generated pulsed field (frequency ω_m and Rabi frequency $2\Omega_m$).

[25–32] but in different contexts. Here we shall give a time-dependent analysis of the FWM scheme in an ultraslow-propagation regime. We shall obtain the analytical expressions of pulsed probe laser, FWM-generated pulse, the corresponding phase shifts, absorption coefficients and group velocities, and the FWM efficiency as well. We shall show that an efficiently generated FWM field can acquire the same ultraslow group velocity and pulse shape of a probe pump and that the maximum FWM efficiency is greater than 25%, orders of magnitude larger than previous four-wave mixing schemes in the ultraslow-propagation regime.

We begin with the Hamiltonian in the interaction picture (taking $\hbar = 1$),

$$H = -\Delta\omega_c|1\rangle\langle 1| - \Delta\omega_p|2\rangle\langle 2| - \Delta\omega_d|3\rangle\langle 3| - (\Omega_c e^{ik_c \cdot r}|2\rangle\langle 1| + \Omega_d e^{ik_d \cdot r}|3\rangle\langle 1| + \text{H.c.}) - (\Omega_p e^{ik_p \cdot r}|2\rangle\langle 0| + \Omega_m e^{ik_m \cdot r}|3\rangle\langle 0| + \text{H.c.}), \quad (1)$$

where $\Delta\omega_p = \omega_p - (\epsilon_2 - \epsilon_0)$ is the single-photon detuning, $\Delta\omega_c = (\omega_p - \omega_c) - (\epsilon_1 - \epsilon_0)$ is the two-photon detuning, $\Delta\omega_d = (\omega_p - \omega_c + \omega_d) - (\epsilon_3 - \epsilon_0)$ is the three-photon detuning, ϵ_j is the energy of the atomic state $|j\rangle$, and ω_n and $2\Omega_n$ ($n = c, d, p, m$) are the frequencies and Rabi frequencies of the relevant fields. Defining the atomic state as $|\Psi\rangle = A_0|0\rangle + A_1 e^{i(\mathbf{k}_p - \mathbf{k}_c) \cdot \mathbf{r}}|1\rangle + A_2 e^{i\mathbf{k}_p \cdot \mathbf{r}}|2\rangle + A_3 e^{i(\mathbf{k}_p - \mathbf{k}_c + \mathbf{k}_d) \cdot \mathbf{r}}|3\rangle$, we then readily from the Schrödinger equation obtain the atomic equations of motion,

$$\frac{\partial A_1}{\partial t} = i(\Delta\omega_c + i\gamma_1)A_1 + i\Omega_d^* A_3 + i\Omega_c^* A_2, \quad (2a)$$

$$\frac{\partial A_2}{\partial t} = i(\Delta\omega_p + i\gamma_2)A_2 + i\Omega_c A_1 + i\Omega_p A_0, \quad (2b)$$

$$\frac{\partial A_3}{\partial t} = i(\Delta\omega_d + i\gamma_3)A_3 + i\Omega_m A_0 + i\Omega_d A_1, \quad (2c)$$

where $\gamma_{1,2,3}$ are added to describe the corresponding decay rates and we have utilized the phase matching condition $\mathbf{k}_m = \mathbf{k}_p - \mathbf{k}_c + \mathbf{k}_d$.

Taking the Fourier transform of Eq. (2) and the wave equations for the pulsed probe field Ω_p and the FWM-

generated field Ω_m , and using the nondepleted ground-state approximation ($A_0 \approx 1$), we obtain

$$(\omega + \Delta\omega_c + i\gamma_1)\beta_1 + \Omega_d^*\beta_3 + \Omega_c^*\beta_2 = 0, \quad (3a)$$

$$(\omega + \Delta\omega_p + i\gamma_2)\beta_2 + \Omega_c\beta_1 = -\Lambda_p, \quad (3b)$$

$$(\omega + \Delta\omega_d + i\gamma_3)\beta_3 + \Omega_d\beta_1 = -\Lambda_m, \quad (3c)$$

$$\frac{\partial\Lambda_p}{\partial z} - i\frac{\omega}{c}\Lambda_p = i\kappa_{02}\beta_2, \quad \frac{\partial\Lambda_m}{\partial z} - i\frac{\omega}{c}\Lambda_m = i\kappa_{03}\beta_3, \quad (4)$$

where β_j , Λ_p , and Λ_m are the Fourier transforms of A_j , Ω_p , and Ω_m , respectively. ω is the Fourier variable and $\kappa_{02(03)} = 2N\omega_{p(m)}|D_{02(03)}|^2/(c\hbar)$ with N and $D_{02(03)}$ being the concentration and dipole moment between states $|0\rangle$ and $|2\rangle$ (3), respectively.

The solution to Eq. (3) is

$$\beta_1 = -\frac{(\omega + \Delta\omega_d + i\gamma_3)\Omega_c^*\Lambda_p + (\omega + \Delta\omega_p + i\gamma_2)\Omega_d^*\Lambda_m}{D}, \quad (5a)$$

$$\beta_2 = -\frac{D_p}{D}\Lambda_p + \frac{\Omega_c\Omega_d^*}{D}\Lambda_m, \quad \beta_3 = \frac{\Omega_c^*\Omega_d}{D}\Lambda_p - \frac{D_m}{D}\Lambda_m, \quad (5b)$$

where $D = D(\omega)$, $D_p = D_p(\omega)$, $D_m = D_m(\omega)$, and

$$D(\omega) = |\Omega_c|^2(\omega + \Delta\omega_d + i\gamma_3) + |\Omega_d|^2(\omega + \Delta\omega_p + i\gamma_2) - (\omega + \Delta\omega_c + i\gamma_1)(\omega + \Delta\omega_p + i\gamma_2)(\omega + \Delta\omega_d + i\gamma_3), \quad (6a)$$

$$D_p(\omega) = |\Omega_d|^2 - (\omega + \Delta\omega_c + i\gamma_1)(\omega + \Delta\omega_d + i\gamma_3), \quad (6b)$$

$$D_m(\omega) = |\Omega_c|^2 - (\omega + \Delta\omega_c + i\gamma_1)(\omega + \Delta\omega_p + i\gamma_2). \quad (6c)$$

Substituting Eq. (5b) into Eq. (4) and making use of the initial condition for the FWM-generated field—i.e., $\Lambda_m(0, \omega) = 0$ —we obtain

$$\Lambda_p(z, \omega) = \frac{\Lambda_p(0, \omega)[U_+e^{izK_-} - U_-e^{izK_+}]}{U_+ - U_-}, \quad (7a)$$

$$\Lambda_m(z, \omega) = \frac{U_+U_- \Lambda_p(0, \omega)[e^{izK_-} - e^{izK_+}]}{U_+ - U_-}, \quad (7b)$$

where $K_{\pm} = K_{\pm}(\omega)$, $U_{\pm} = U_{\pm}(\omega)$, and

$$K_{\pm}(\omega) = \frac{\omega}{c} + \frac{-[\kappa_{03}D_m(\omega) + \kappa_{02}D_p(\omega)] \pm \sqrt{G(\omega)}}{2D(\omega)} = K_{\pm}(0) + K_{\pm}^{(1)}\omega + O(\omega^2), \quad (8a)$$

$$U_{\pm}(\omega) = \frac{\kappa_{02}D_p(\omega) - \kappa_{03}D_m(\omega) \pm \sqrt{G(\omega)}}{2\kappa_{02}\Omega_c\Omega_d^*} = W_{\pm} + O(\omega), \quad (8b)$$

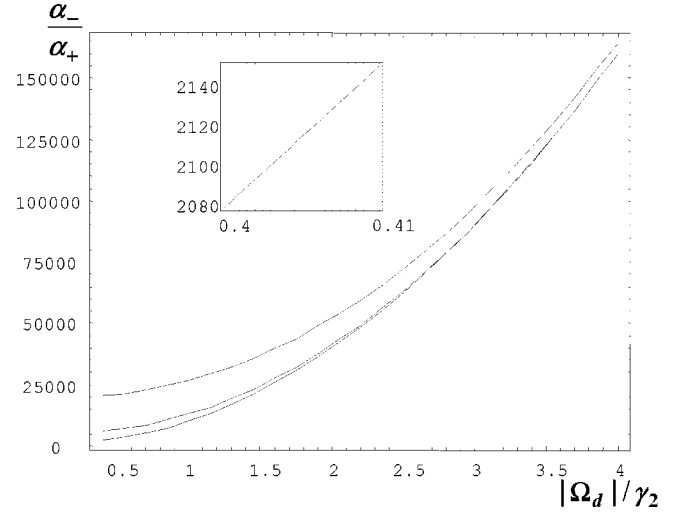


FIG. 2. The ratio of absorption coefficients α_-/α_+ versus $|\Omega_d|/\gamma_2$ for $|\Omega_c|/\gamma_2=2$ (uppermost), 1 (middle), and 0.4 (lowest). The inset shows the lowest curve $|\Omega_c|/\gamma_2=0.4$ for $|\Omega_d|/\gamma_2$ in the small interval $[0.4, 0.401]$. The other parameters are $\kappa_{02}=\kappa_{03}$, $\gamma_1/\gamma_2=10^{-4}$, $\gamma_3/\gamma_2=2.5/1.2$, $\Delta\omega_c=\Delta\omega_p=0$, and $\Delta\omega_d=0.02\gamma_2$.

$$W_{\pm} = U_{\pm}(0),$$

with $G(\omega) = [\kappa_{03}D_m(\omega) - \kappa_{02}D_p(\omega)]^2 + 4\kappa_{03}\kappa_{02}|\Omega_c|^2|\Omega_d|^2$.

The analytical expressions of the pulsed fields are still complicated in order to perform the inverse Fourier transform, but much physical insight can be gained by seeking their approximated inverse Fourier transform with the approximation of neglecting both $O(\omega)$ terms in U_{\pm} and $O(\omega^2)$ terms in K_{\pm} (the approximation is fairly accurate for typical parameters considered here; see Fig. 3). Then it is straightforward to obtain

$$\Omega_p(z, t) = \frac{W_+\Omega_p(\eta_-)e^{izK_-(0)} - W_-\Omega_p(\eta_+)e^{izK_+(0)}}{W_+ - W_-}, \quad (9a)$$

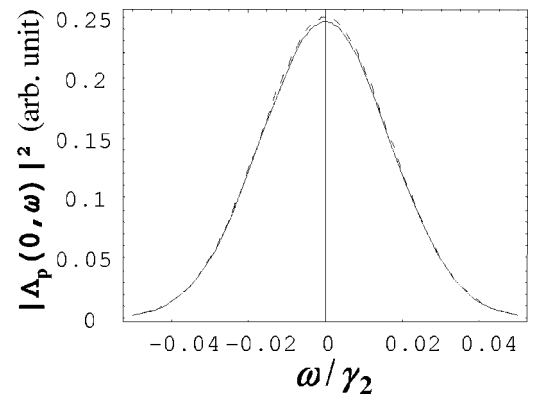


FIG. 3. $|\Lambda_p(0, \omega)|^2$ versus ω/γ_2 with $\Lambda_p(0, \omega) = \Omega_{p0}\tau\sqrt{\pi}\exp[-(\omega\tau)^2/4] \Leftrightarrow \Omega(0, t) = \Omega_{p0}\exp[-t^2/\tau^2]$. The solid-line curve represents the exact solution (7b) while the dashed-line curve denotes the approximated solution by neglecting the $\exp(iK_{\pm}z)$ term and taking $U_{\pm} \approx W_{\pm}$ and $K_{\pm} \approx K_{\pm}(0) + K_{\pm}^{(1)}\omega$ in Eq. (7b). The parameters are $\tau=10^{-6}$ s and $\Omega_c=\Omega_b=\gamma_2$.

$$\Omega_m(z,t) = \frac{W_+ W_- [\Omega_p(\eta_-) e^{izK_-^{(0)}} - \Omega_p(\eta_+) e^{izK_+^{(0)}}]}{W_+ - W_-}, \quad (9b)$$

where $\Omega_p(t) \equiv \Omega_p(z=0, t)$ is the pump field at $z=0$, $\eta_{\pm} = t - z/V_{g\pm}$, $W_{\pm} = U_{\pm}(0)$, the group velocities $V_{g\pm}$ are determined by $1/V_{g\pm} = \text{Re}[K_{\pm}^{(1)}]$, $\text{Re}[K_{\pm}(0)]$ denote the phase shifts per unit length, and $\text{Im}[K_{\pm}(0)] \equiv \alpha_{\pm}$ are absorption coefficients.

For the typical parameters and conditions for hyperfine-split alkaline-earth-metal atom D lines and the pump lasers, it is found that the absorption coefficient α_- is usually much greater than another absorption coefficient α_+ . For instance, Fig. 2 shows the ratio α_-/α_+ for the parameters $\Gamma_1 = 2\gamma_1 \approx 1.2 \times 10^4 \text{ s}^{-1}$, $\Gamma_2 = 2\gamma_2 \approx 1.2 \times 10^8 \text{ s}^{-1}$, and $\Gamma_3 = 2\gamma_3 \approx 2.5 \times 10^8 \text{ s}^{-1}$, typical for transitions in hyperfine-split Na D lines [19]. The key consequence of this result is that under these conditions one of the components in Eqs. (9a) and (9b) decays much faster than the other. Consequently, after a short characteristic propagation distance one has

$$\Omega_p(z,t) = \frac{W_-}{W_- - W_+} \Omega_p \left(t - \frac{z}{V_g} \right) e^{iz\phi - z\alpha}, \quad (10a)$$

$$\Omega_m(z,t) = \frac{W_+ W_-}{W_- - W_+} \Omega_p \left(t - \frac{z}{V_g} \right) e^{iz\phi - z\alpha}, \quad (10b)$$

where $V_g = V_{g+} = 1/\text{Re}[K_+^{(1)}]$ is the group velocity, $\alpha = \text{Im}[K_+(0)]$ denotes absorption coefficient, and $\phi = \text{Re}[K_+(0)]$ represents phase shift per unit length. The analytical expressions of the quantities $K_+(0)$ and $K_+^{(1)} = [\partial K_+(\omega)/\partial \omega]_{\omega=0}$ can readily be obtained through $K_+(\omega)$ given in Eq. (8a).

Figure 3 shows that Eqs. (10) represent a very accurate approximate solution for typical transitions in hyperfine-split Na D lines and appropriate conditions for the pump lasers. Figure 4 illustrates that the probe field and the FWM-generated field as given by Eq. (10) travel with an ultraslow

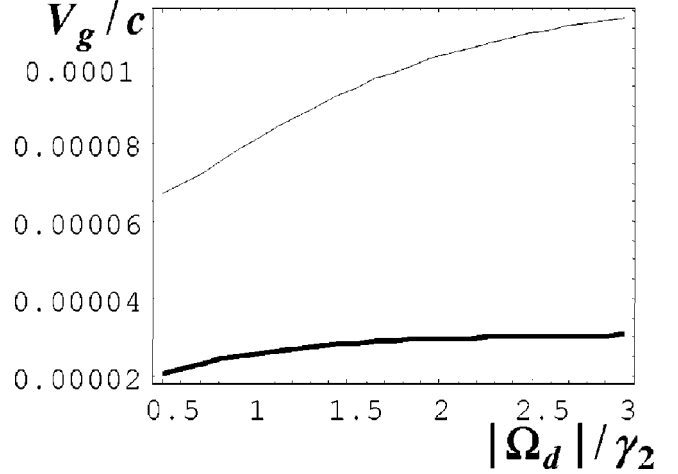


FIG. 4. The relative group velocity V_g/c versus $|\Omega_d|/\gamma_2$ with $\Omega_c = 0.5\gamma_2$ (thick line) and $\Omega_c = \gamma_2$ (thin line). The parameters $\kappa_{02} = \kappa_{03} = 2 \times 10^9 \text{ cm}^{-1} \text{ s}^{-1}$, $\gamma_1/\gamma_2 = 10^{-4}$, $\gamma_3/\gamma_2 = 2.5/1.2$, $\Delta\omega_c = \Delta\omega_p = 0$, $\Delta\omega_d = 0.02\gamma_2$, and $\gamma_2 \approx 0.6 \times 10^8 \text{ s}^{-1}$.

group velocity ($V_g/c \sim 10^{-4} - 10^{-5}$ for the parameters given in Fig. 4). It is possible to further reduce the already small group velocity by increasing κ_{02} and κ_{03} .

Equation (10) demonstrates that the FWM-generated field and the probe field can, after a short characteristic distance, travel through the cold atom medium with the same temporal profile and ultraslow group velocity. We define the FWM efficiency η as the ratio of the energy of the output FWM-generated field and the energy the input probe field—i.e., $\eta = |E_m^{(out)}/E_p^{(in)}|^2$. Here $E_m^{(out)}$ is the electric field E_m ($|E_m|^2 = 4\hbar^2 |\Omega_m|^2 / |D_{03}|^2$) of the FWM-generated field at the exit $z = L$ and $E_p^{(in)}$ is the electric field E_p ($|E_p|^2 = 4\hbar^2 |\Omega_p|^2 / |D_{02}|^2$) of the probe field at the entrance $z=0$. According to Eq. (10), the efficiency has the form

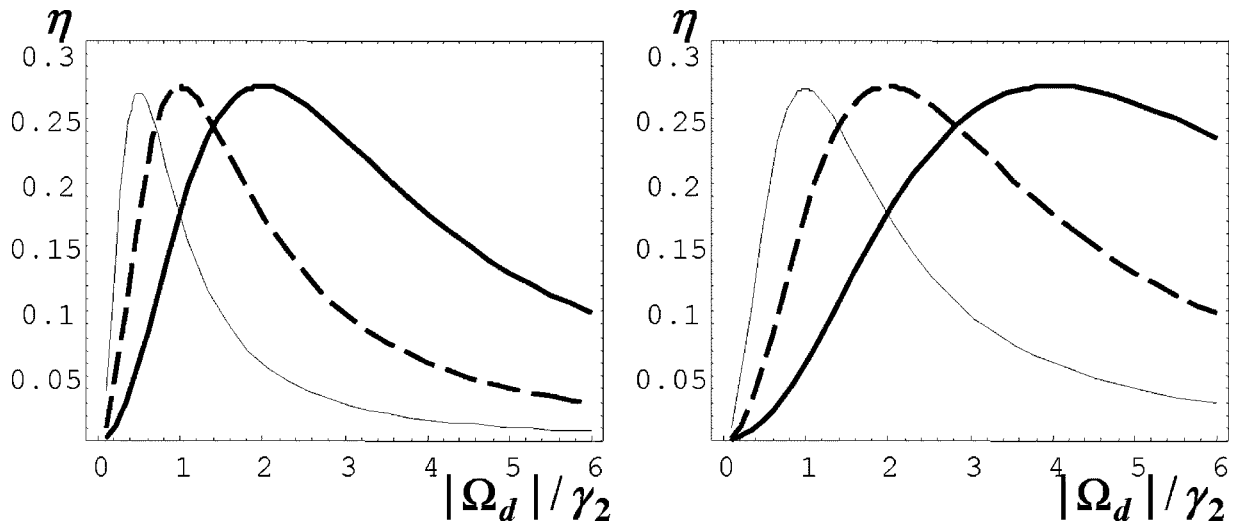


FIG. 5. FWM efficiency η versus $|\Omega_d|/\gamma_2$ for $|\Omega_c|/\gamma_2 = 2$ (thick solid line), 1 (dashed line), and 0.5 (thin solid line). The left (right) panel has $\kappa_{02} = \kappa_{03} = 2 \times 10^9 \text{ cm}^{-1} \text{ s}^{-1}$ ($\kappa_{03} = 4\kappa_{02} = 2 \times 10^9 \text{ cm}^{-1} \text{ s}^{-1}$). The other parameters for both panels are $\gamma_1/\gamma_2 = 10^{-4}$, $\gamma_3/\gamma_2 = 2.5/1.2$, $\Delta\omega_c = \Delta\omega_p = 0$, $\Delta\omega_d = 0.02\gamma_2$, $\gamma_2 \approx 0.6 \times 10^8 \text{ s}^{-1}$, $\omega_m = 1.1\omega_p$ and $L = 1 \text{ cm}$.

$$\eta \approx \frac{\omega_m \kappa_{02} \kappa_{03} |\Omega_c|^2 |\Omega_d|^2 \exp(-2\alpha L)}{\omega_p (|F|^2 + 4\kappa_{03} \kappa_{02} |\Omega_c|^2 |\Omega_d|^2)}, \quad (11)$$

where $F = \kappa_{03} |\Omega_c|^2 - \kappa_{02} |\Omega_d|^2 + (\Delta\omega_c + i\gamma_1) [\kappa_{02} (\Delta\omega_d + i\gamma_3) - \kappa_{03} (\Delta\omega_p + i\gamma_2)] \approx \kappa_{03} |\Omega_c|^2 - \kappa_{02} |\Omega_d|^2$ and $\alpha = \text{Im}[K_+(0)]$ is determined by Eq. (8a). In writing Eq. (11), we have made use of the relation $\kappa_{02} \omega_m / (\kappa_{03} \omega_p) = |D_{02}/D_{03}|^2$. It is seen from Eq. (11) that the maximum efficiency η_{max} is achieved at $\kappa_{03} |\Omega_c|^2 \approx \kappa_{02} |\Omega_d|^2$, and we thus have

$$\eta_{max} \approx \frac{\omega_m}{4\omega_p} e^{-2\alpha L}. \quad (12)$$

Figure 5 shows that the efficiency versus the amplitude $|\Omega_d|$ of the cw pump field d for several amplitude values of another cw pump field. From this figure, it is seen that the maximum efficiency is indeed achieved at around $\kappa_{03} |\Omega_c|^2 \approx \kappa_{02} |\Omega_d|^2$ and the maximum efficiency is about $\omega_m / \omega_p \times 25\%$ even for a sample thickness as large as $L=1$ cm for the typical transition parameters of hyperfine-split Na D lines.

It is pointed out that one frequently in the previous literature adopts another definition of the efficiency defined as $\eta^{(\Omega)} = |\Omega_m^{(out)} / \Omega_p^{(in)}|^2 \equiv \eta |D_{03}/D_{02}|^2$. In particular the maximum efficiency $\eta^{(\Omega)}$ in our case, according to Eq. (12), has the form

$$\eta_{max}^{(\Omega)} = \eta_{max} \frac{|D_{03}|^2}{|D_{02}|^2} \approx \frac{\omega_m |D_{03}|^2}{4\omega_p |D_{02}|^2} e^{-2\alpha L}. \quad (13)$$

From this expression and Fig. 5, it is readily seen that the maximum efficiency $\eta^{(\Omega)}$ can be much greater than 100% when the two dipole moments satisfy $|D_{03}| \gg 2|D_{01}|$ in the cases of zero or small detunings, as compared with the maximum efficiency $\eta_{max}^{(\Omega)}$ never exceeding 25% in the cases of zero or small detunings in the previous studies [3,4,20], while the FWM experimental data [26] have indeed shown the situations of $\eta_{max}^{(\Omega)} \geq 100\%$.

In summary, we have analyzed the four-wave mixing in an ultraslow-propagation regime in a double- Λ system with a time-dependent approach. We have derived the analytical expressions of the pulsed probe laser, FWM-generated pulse, phase shifts and absorption coefficients, group velocities, and FWM efficiency. With these analytical expressions, we show that an efficiently generated FWM field can acquire the same ultraslow group velocity ($V_g/c \sim 10^{-4} - 10^{-5}$) and pulse shape of a probe pump and that the maximum FWM efficiency is greater than 25%, which is orders of magnitude larger than previous four-wave mixing schemes in the ultraslow-propagation regime.

Before ending, we would like to mention the key points of the present study. One of the major differences between our FWM scheme with those previous studies in the same double- Λ configuration lies in the fact that previous studies [25–32] considered all four waves as cw waves while we treat two of them (the probe and FWM fields) as pulsed fields interacting with each other in a time-dependent way. It is important that such a time-dependent treatment results in two coupled equations, leading to the two modes (K_{\pm} modes) of greatly different absorptions in the typical parameters con-

sidered here. The high efficiency originates from the fact that one of the two modes (the K_- mode) is heavily damped compared with another mode (the K_+ mode), proving the concept of the matched pulses [26]. Another important difference is that the previous cw treatments of the FWM in the double- Λ configuration are not in the ultraslow regime. One drawback of the cw treatment is that it cannot *properly* include the coupling of the two fields and hence cannot obtain the correct group velocities (notice that each of the two modes, the K_{\pm} modes, contains both the probe and FWM fields but differs from either the probe or the FWM fields and the group velocities of the two modes differ from those of the probe and FWM fields themselves when the coupling is omitted), while our time-dependent treatment correctly accounts for such a coupling. In this way, we have investigated the FWM scheme in a double- Λ configuration in the *ultraslow group regime* and shown that there exists the phenomenon of matched pulses in the ultraslow-propagation regime.

The phenomenon of matched pulses in our scheme is readily seen to come from multiphoton quantum interference. For instance, the interference of the two paths $|0\rangle \rightarrow |2\rangle \rightarrow |1\rangle \rightarrow |3\rangle$ and $|0\rangle \rightarrow |3\rangle$ leads to the relation $\Omega_m = -\Omega_d A_1$ from Eqs. (5) and (7) when the phenomenon takes place. This relation and Eq. (2c) imply that the probability amplitude A_3 is nearly unchanged then and hence the FWM field ceases to increase due to the multiphoton quantum interference. It is pointed out that the phenomenon of matched pulses greatly simplifies the calculation of the expression of the efficiency (notice that the efficiency defined as the ratio of the energy of the output FWM-generated field and the energy the input probe field usually needs integrations over either time or frequency intervals depending on whether the fields are given in terms of the time or the frequency variables) because the involved integrations (in both the denominator and nominator) have canceled out each other when the two pulses have the same temporal shape.

Adapting the Schrödinger formalism with decay rates included, just as done before by some authors [19,26,33,34], permits us to obtain simple analytical expressions. It can readily be checked by numerical computations that the results of such a treatment are essentially the same as those from the usual density matrix formalism under the condition that all atoms be initially in the ground state $|0\rangle$. For instance, it can readily be seen that when we take $\Omega_d = \Omega_m = 0$, corresponding to the standard electromagnetically induced transparency (EIT) in the (single) Λ configuration, Eq. (5) will lead to the standard EIT results [33] in the (single) Λ configuration. When taking $\Omega_m = 0$ and $\kappa_{03} = 0$ as well as considered the cw situation (simply taking $\omega = 0$ in all results), it can readily be shown that our results become those in the previous study on the same atom and field system with a cw treatment [34].

Finally, although we have plotted figures and discuss the results by choosing the typical parameters and conditions for typical transitions of hyperfine-split Na D lines and the pump lasers, we have actually done the same numerical calculations (not shown here) for typical parameters and conditions for typical transitions of hyperfine-split Rb D lines and pump lasers, and find similar conclusions. We believe that similar conclusions should also be suitable for other alkaline-earth-metal atoms D lines as well.

The work is supported in part by the NSF of China (Grant Nos. 60478029, 90103026, 10125419, and 10121503) and by the National Fundamental Research Program of China, Grant

No. 2001CB309310. Y.W. thanks Dr. L. Deng for a stimulating discussion.

-
- [1] S. E. Harris and L. V. Hau, *Phys. Rev. Lett.* **82**, 4611 (1999).
 [2] M. D. Lukin and A. Imamoglu, *Phys. Rev. Lett.* **84**, 1419 (2000).
 [3] L. Deng, M. Kozuma, E. W. Hagley, and M. G. Payne, *Phys. Rev. Lett.* **88**, 143902 (2002).
 [4] Y. Wu, J. Saldana, and Y. Zhu, *Phys. Rev. A* **67**, 013811 (2003).
 [5] Y. Wu, L. Wen, and Y. Zhu, *Opt. Lett.* **28**, 631 (2003).
 [6] Y. Zhu, J. Saldana, L. Wen, and Y. Wu, *J. Opt. Soc. Am. B* **21**, 806 (2004).
 [7] L. Deng and M. G. Payne, *Phys. Rev. A* **68**, 051801(R) (2003).
 [8] C. Dorman, I. Kucukkara, and J. P. Marangos, *Phys. Rev. A* **61**, 013802 (1999).
 [9] E. Paspalakis and P. L. Knight, *Phys. Rev. A* **66**, 015802 (2002).
 [10] L. Deng and M. G. Payne, *Phys. Rev. Lett.* **91**, 243902 (2003).
 [11] M. G. Payne and L. Deng, *Phys. Rev. Lett.* **91**, 123602 (2003).
 [12] Y. Wu and L. Deng, *Opt. Lett.* **29**, 1144 (2004).
 [13] S. F. Yelin, V. A. Sautenkov, M. M. Kash, G. R. Welch, and M. D. Lukin, *Phys. Rev. A* **68**, 063801 (2003).
 [14] A. S. Zibrov, C. Y. Ye, Y. V. Rostovsev, A. B. Matsko, and M. O. Scully, *Phys. Rev. A* **65**, 043817 (2002).
 [15] A. B. Matsko, I. Novikova, G. R. Welch, and M. S. Zubairy, *Opt. Lett.* **28**, 96 (2003).
 [16] M. D. Lukin, P. R. Hemmer, and M. O. Scully, *Adv. At., Mol., Opt. Phys.* **42**, 347 (2000).
 [17] M. Yan, E. Riskey, and Y. Zhu, *Phys. Rev. A* **64**, 043807 (2001); H. Kang, G. Hernandez, and Y. Zhu, *Phys. Rev. Lett.* **93**, 073601 (2004).
 [18] Y. Wu, M. G. Payne, E. W. Hagley, and L. Deng, *Opt. Lett.* **29**, 2294 (2004).
 [19] H. Schmidt and A. Imamoglu, *Opt. Lett.* **21**, 1936 (1996).
 [20] M. G. Payne and L. Deng, *Phys. Rev. A* **65**, 063806 (2002).
 [21] H. Kang and Y. Zhu, *Phys. Rev. Lett.* **91**, 093601 (2003).
 [22] B. S. Ham, M. S. Shahriar, and R. Hemmer, *Opt. Lett.* **24**, 86 (1999).
 [23] A. F. Huss, N. Peer, R. Lammegger, E. A. Korsunsky, and L. Windholz, *Phys. Rev. A* **63**, 013802 (2000); A. K. Popov, V. V. Kimberg, and T. F. Gorge, *ibid.* **69**, 043816 (2004).
 [24] S. Wang, D. G. Ducreay, R. Pina, M. Yan, and Y. Zhu, *Phys. Rev. A* **61**, 033805 (2000).
 [25] E. A. Korsunsky and D. V. Kosachiov, *Phys. Rev. A* **60**, 4996 (1999).
 [26] A. J. Merriam, S. J. Sharpe, M. Shverdin, D. Manuszak, G. Y. Yin, and S. E. Harris, *Phys. Rev. Lett.* **84**, 5308 (2000).
 [27] B. Lu, W. H. Burkett, and M. Xiao, *Opt. Lett.* **23**, 804 (1998).
 [28] B. S. Ham, M. S. Shahriar, M. K. Kim, and P. R. Hemmer, *Opt. Lett.* **22**, 1849 (1997).
 [29] M. Johnsson and M. Fleischhauer, *Phys. Rev. A* **68**, 023804 (2003).
 [30] F. L. Kien and K. Hakuta, *Phys. Rev. A* **69**, 043811 (2004).
 [31] M. D. Lukin, A. B. Matsko, M. Fleischhauer, and M. O. Scully, *Phys. Rev. Lett.* **82**, 1847 (1999).
 [32] A. S. Zibrov, M. D. Lukin, and M. O. Scully, *Phys. Rev. Lett.* **83**, 4049 (1999).
 [33] M. O. Scully and M. S. Zubairy, *Quantum Optics* (Cambridge University Press, Cambridge, England, 1997), Chap. 7.
 [34] S. E. Harris and Y. Yamamoto, *Phys. Rev. Lett.* **81**, 3611 (1998).